IEEE Access
Multidisciplinary | Rapid Review | Open Access Journal

Received July 2, 2020, accepted July 11, 2020, date of publication July 14, 2020, date of current version July 24, 2020.

Digital Object Identifier 10.1109/ACCESS.2020.3009267

An Adaptive Strategy to Compensate Nonlinear Effects of Voltage Source Inverters Based on Artificial Neural Networks

TAO LIU[1], QIDONG LI[1], QIAOLING TONG[1], (Member, IEEE), QIAO ZHANG[2], (Member, IEEE), AND KAN LIU[3], (Senior Member, IEEE)

[1]School of Optical and Electronic Information, Huazhong University of Science and Technology, Wuhan 430074, China
[2]School of Automation, Wuhan University of Technology, Wuhan 430074, China
[3]College of Mechanical and Vehicle Engineering, Hunan University, Changsha 410082, China

Corresponding author: Qiaoling Tong (tongqiaoling@hust.edu.cn)

This work was supported by the National Natural Science Foundation of China under Grant 61640311 and Grant 61701184.

ABSTRACT In motor drives, distortions of phase voltages and currents are often caused by nonlinear effects of inverters such as dead time, turn-on delay, turn-off delay and voltage drop of power devices. To eliminate these distortions, the dead-time compensation voltage is usually investigated. Furthermore, the relationship between the dead-time compensation voltage and phase currents is nonlinear, which is related to not only the parameters mentioned above, but also the snubber and parasitic capacitance of inverters. A nonlinear function is constructed to model the nonlinear relationship in this paper. To identify the nonlinear function, a method based on artificial neural networks is proposed without inverter parameters. According to the criterion that the trajectory of voltage vector in α-β coordinate system is a circle, an adaptive law is constructed to modify the parameters of the nonlinear function. Therefore, the nonlinear dead-time compensation voltage model is obtained accurately, where the distortions of voltages and currents are reduced without any additional hardware. Applying this method to the current predictive control, the bandwidth of a current loop is increased by 500Hz. Effectiveness of the method is verified by experiments.

INDEX TERMS Inverter nonlinear effects, artificial neural network, nonlinear dead-time compensation model.

I. INTRODUCTION

Pulse-width-modulated (PWM) based voltage source inverters (VSIs) are widely used in motor drives because of its high efficiency, low harmonic component output, and easy to be controlled. In the control of VSIs, a dead time, inserted between the switching signals of each phase leg, is adopted to prevent the conduction overlap. However, nonlinear effects of inverters such as dead time, turn-on delay, turn-off delay and voltage drop of power devices induce a voltage mismatch between actual phase voltages and reference voltages. This mismatch leads to the distortions of three-phase currents. Furthermore, the actual phase voltages need to be obtained accurately in some applications, such as motor parameter identification and current predictive control. Nevertheless, additional filter circuits are required to measure the actual phase voltages from the pulse output voltage of VSIs, where a sampling delay is introduced. To avoid these problems, instead of using the actual phase voltages, the reference voltages are often used for calculations. However, the control performance and accuracy of parameter identification are degraded by the voltage mismatch.

To solve these problems led by voltage mismatch, some offline methods are proposed by investigating the dead-time compensation voltage. According to the phase current polarity, the dead-time voltage is compensated directly [1], [2]. Since this method often leads to wrong judgement of current polarity, the sector of current vector is utilized to judge the current polarity indirectly [3]. To avoid the compensation failure in the current zero-crossing region by the above strategies, a trapezoidal form of wave compensation strategy is proposed [4]. In these methods, the relationship between the dead-time compensation voltage and phase currents is considered as an ideal linear function. However, this relationship is nonlinear considering the parasitic capacitance of power devices, which needs to be charged or discharged during the switching

The associate editor coordinating the review of this manuscript and approving it for publication was Atif Iqbal.

process [5]–[7]. In [6], a piecewise compensation method was proposed to match the nonlinear relationship. In the mentioned literatures, some parasitic parameters of inverters are required. Since these parameters vary with circuit state, they are often regarded as an approximate value. It constrains the accuracy of compensation result in offline methods.

In order to improve the accuracy of compensation result, some online compensation methods are proposed, such as disturbance observers [8]–[11], d-axis voltage compensation methods [12]–[15], sixth harmonic eliminated methods [16]–[21], current predictive control methods [22]–[24], and repeating controllers [25]–[28]. Regarding the dead-time voltage as a voltage disturbance, a disturbance observer is constructed to estimate the compensation voltage according to the voltage equation [8]. In [12], an Adaline estimator is proposed to estimate the dead-time compensation voltage according to the d-axis voltage characteristics, where the voltage fluctuation is mainly caused by the dead-time voltage. To compensate the voltage distortions of a specific sixth harmonic in d-q coordinate system, an active filter utilizing the least-mean-square (LMS) method is proposed [17], [18]. In [24], the error between the predictive current and actual current is used to estimate the dead-time compensation voltage. According to the periodic behavior of the dead-time voltage, a repeating controller is constructed [25]. In these online methods, some parameters of motors are required, which are difficult to be obtained accurately. Besides, they can be affected by the operating conditions, which degrades the voltage compensation effect. Furthermore, the relationship between the dead-time compensation voltage and the phase currents is simplified as a sign function. Since the relationship is a complex model, this simplification leads to the discontinuities of compensation voltages in the current zero-crossing region, which fails to minimize the voltage mismatch. To identify complex models without system parameters, artificial neural network (ANN) algorithms are widely proposed [29]–[31]. Therefore, the ANN-based method is an alternative to achieve the accurate compensation model of dead-time voltage and improve the compensation accuracy.

To improve the compensation effect to the voltage mismatch and current distortions, an online compensation method based on ANN is proposed in this paper. Firstly, a nonlinear function is constructed to model the relationship between the dead-time compensation voltage and phase currents. The parameter of the nonlinear function is utilized to describe the effect to different parameters of inverters. Secondly, the nonlinear function is identified by an ANN structure without inverter parameters, where an adaptive law is constructed to modify the parameters of the nonlinear function. The characteristics of the voltage vector in α-β coordinate system is analyzed, where the trajectory of the voltage vector is a circle without considering the voltage mismatch. According to this characteristic, an adaptive law is constructed by modifying the dead-time compensation voltage to make the trajectory of the voltage vector after compensation approach a circle. Therefore, the nonlinear function of dead-time compensation voltage is identified online. Moreover, the voltage mismatch is reduced and the actual phase voltages are obtained accurately without adding any hardware. Finally, applying this method to the current predictive control, the bandwidth of the current loop is increased by 500Hz. The current distortions due to the voltage mismatch of reference voltages and actual phase voltages are also reduced.

The rest of this paper is organized as follows. Section II analyzes the nonlinear relationship between the dead-time compensation voltage and phase currents. Section III proposes a nonlinear identification model based on ANN and introduces the implementation process of the compensation method. Section IV verifies the effectiveness of the algorithm through experiments. Section V summarizes this article.

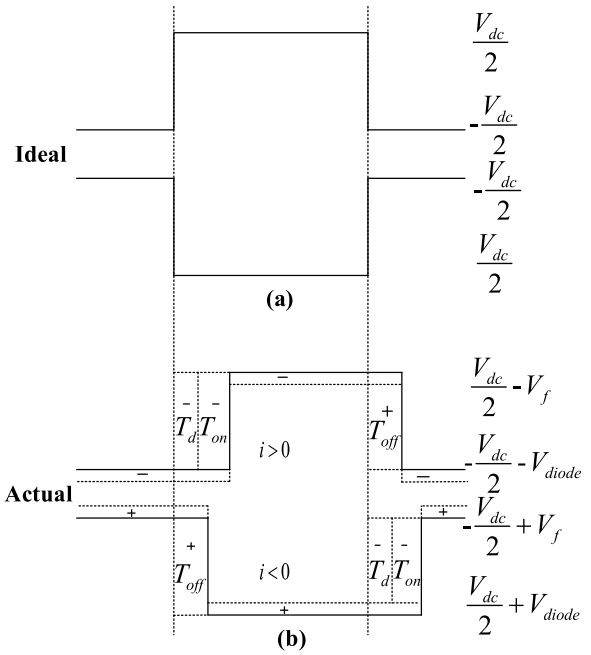

FIGURE 1. (a) Ideal PWM signal. (b) Actual PWM signal considering the nonlinear effects of inverters.

II. NONLINEAR DEAD-TIME VOLTAGE MODEL

The inverter nonlinear effects such as dead time, turn-on delay, turn-off delay and voltage drop of power devices cause a voltage mismatch between the actual phase voltages and the reference voltages. The dead-time voltage is usually investigated to compensate the voltage mismatch. The relationship between the dead-time compensation voltage and phase currents is nonlinear, which is analyzed as follows. The PWM signals of power devices are shown in Fig. 1. The compensation voltages are expressed as (1) according to Fig. 1 [18]:

$$\Delta V = V_d sign(i), sign(i) = \begin{cases} -1, & i < 0 \\ 1, & i > 0, \end{cases} \tag{1}$$

where sign(i) is the sign function. V_d *is* the magnitude of the compensation voltage, which is defined as:

$$V_d = \frac{T_d + T_{on} - T_{off}}{T_s} V_{dc} + \frac{V_f + V_{diode}}{2}, \tag{2}$$

where V_{dc} is the DC link, V_f is the voltage drop of power devices, V_{diode} is the voltage drop of diodes. T_d is the dead time, T_{on} is the turn-on delay, T_{off} is the turn-off delay, T_s is the period of PWM.

Therefore, the compensation voltages in a-b-c coordinate system are obtained as:

$$\begin{cases} \Delta V_a = \dfrac{V_d}{3}(2sign(i_a) - sign(i_b) - sign(i_c)) \\ \Delta V_b = \dfrac{V_d}{3}(2sign(i_b) - sign(i_a) - sign(i_c)) \\ \Delta V_c = \dfrac{V_d}{3}(2sign(i_c) - sign(i_b) - sign(i_a)), \end{cases} \tag{3}$$

where i_a, i_b, and i_c are the phase currents.

Instead of the sign function used in (3), (4) is constructed in this paper:

$$f\,(i) = \frac{2}{1 + e^{-w*i}} - 1, \tag{4}$$

where w is the weight value of this function. Equation (4) is constructed according to the characteristics of the sign function and the transfer function, which is usually used in ANN. When w is set to 7 as an example, the waveform of the proposed nonlinear function is shown in Fig. 2. However, this value of w is related to the parameters of inverters. In different inverter systems, this value needs to be identified.

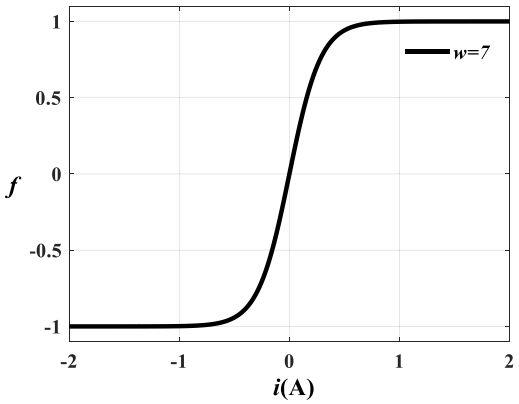

FIGURE 2. The waveform of the proposed function (w = 7).

The compensation voltages ΔV_α, ΔV_β in α-β axes are obtained as (5) by using the coordinate transformation, (3), and (4):

$$\begin{cases} \Delta V_\alpha = \dfrac{V_d}{3}(2f(i_a) - f(i_b) - f(i_c)) \\ \Delta V_\beta = \dfrac{\sqrt{3}\,V_d}{3}(f(i_b) - f(i_c)). \end{cases} \tag{5}$$

Fig. 3 shows the comparison of the compensation voltages with the sign function and the proposed function. The compensation voltages using the proposed function change with the phase currents continuously in the current zero-crossing region. It is more consistent with the actual nonlinear effects of inverters. Since the parameter of the proposed nonlinear function is related to inverter parameters, it needs to be identified online.

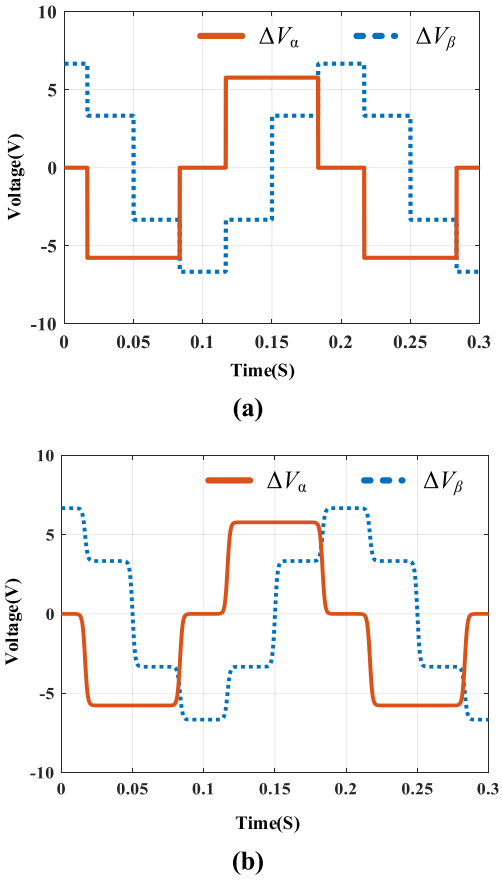

FIGURE 3. The compensation voltage in α-β coordinate system (a) using the sign function and (b) using the proposed function.

III. PROPOSED DEAD-TIME VOLTAGE COMPENSATION METHOD

To identify the nonlinear model of dead-time compensation voltage online, an ANN-based method is proposed. And the compensation method aims to:

- Constructing a nonlinear function to model the complex relationship between the dead-time compensation voltage and phase currents.
- Identifying the nonlinear function online by an ANN method without inverter parameters.

The process of the proposed method is shown as follows: Firstly, an ANN structure is constructed to identify the nonlinear function. Secondly, the maximum compensation voltage is obtained by a two-step voltage method. Thirdly, an adaptive law to modify the parameter of nonlinear function is proposed according to the characteristics of voltage in α-β coordinate system. Finally, applying the compensation method, the current predictive control is performed.

A. ANN MODEL

After the nonlinear function of the dead-time voltage and phase currents is constructed, an ANN structure is proposed to identify the nonlinear function online. In practical, the value of reference voltage vector changes slowly. There-

fore, without considering the nonlinear effects of inverters, the magnitude of reference voltage vector is a constant value in a small duration. However, due to the influence of the dead-time voltage, the amplitude of reference voltage vector is fluctuated periodically. According to this characteristic, a three-inputs and one-output ANN structure is constructed to identify the nonlinear function of the dead-time voltage in α-β coordinate system. Fig. 4 shows the ANN structure. The phase currents are used as input variables, while the magnitude of reference voltage vector is used as the output variable. Without external references, this ANN structure recognizes eigen trend through a self-reference.

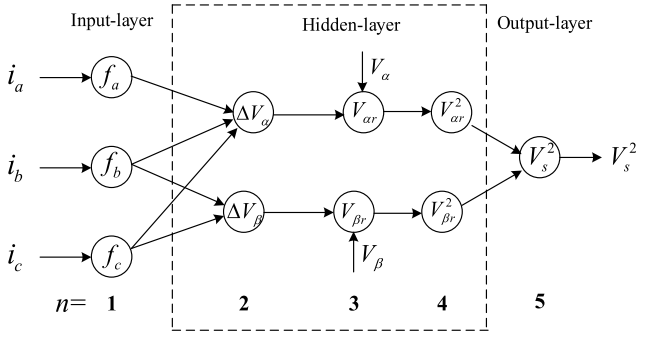

FIGURE 4. The three-inputs and one-output ANN structure.

The ANN structure is described by the following two equations:

$$u_j(n+1) = \sum_i w_{ij}(n+1)Y_i(n) + d_j(n+1), \tag{6}$$

$$Y_j(n+1) = f[u_j(n+1)], \tag{7}$$

where $u_j(n+1)$ is the input of j^{th} neuron in the $n+1^{\text{th}}$ layer, $w_{ij}(n+1)$ is the weight between j^{th} neuron and i^{th} neuron in the $n+1^{\text{th}}$ layer. $d_j(n+1)$ is the threshold of j^{th} neuron in the $n+1^{\text{th}}$ layer, $f[.]$ is the input-output function, $Y_j(n+1)$ is the output of j^{th} neuron in the $n+1^{\text{th}}$ layer. In the proposed neural network structure, the weights and input-output functions are given in Table 1.

It can be seen from Table 1 that w_a, w_b, w_c, and V_d are unknown. V_d will be identified by a two-step voltage method, and the others are identified by the proposed ANN algorithm. Therefore, the maximum dead-time compensation voltage and an adaptive law are required to identify the nonlinear function of dead-time voltage.

B. CALCULATION OF MAXIMUM DEAD-TIME COMPENSATION VOLTAGE BASED ON TWO-STEP VOLTAGE METHOD

As mentioned before, the maximum dead-time compensation voltage is required. To obtain the maximum dead-time compensation voltage, a two-step voltage method is utilized in this section. When the motor is at standstill, two different voltage vectors are output and recorded as $V_{\beta 1}$ and $V_{\beta 2}$. At the same time, the steady-state currents are measured as $i_{\beta 1}$ and $i_{\beta 2}$. Then the following equations are obtained according to the voltage equation:

$$\begin{cases} V_{\beta 1} = Ri_{\beta 1} + \Delta V_{\beta 1} \\ V_{\beta 2} = Ri_{\beta 2} + \Delta V_{\beta 2}, \end{cases} \tag{8}$$

where R is the stator resistance. For simplification, V_α is often set to zero.

TABLE 1. Weights and input-output functions of the ANN.

Layer		Weight			Input-output function
1	$i \backslash j$	1	2	3	$f(u) = \frac{2}{1+e^{-u}} - 1$
	1	w_a	0	0	
	2	0	w_b	0	
	3	0	0	w_c	
2	$i \backslash j$	1		2	$f(u) = u$
	1	$2V_d/3$		0	
	2	$-V_d/3$		$\sqrt{3}V_d/3$	
	3	$-V_d/3$		$-\sqrt{3}V_d/3$	
3	$i \backslash j$	1		2	$f(u) = u$
	1	-1		0	
	2	0		-1	
4	$i \backslash j$	1		2	$f(u) = u^2$
	1	1		0	
	2	0		1	
5	$i \backslash j$	1			$f(u) = u$
	1	1			
	2	1			

According to (5), when $i_{\beta 1}$, $i_{\beta 2}$ are large enough, $\Delta V_{\beta 1}$ is equal to $\Delta V_{\beta 2}$. Therefore, the magnitude of dead-time compensation voltage is calculated as:

$$V_d = \frac{\sqrt{3}}{2}\left(\frac{V_{\beta 2} i_{\beta 1} - V_{\beta 1} i_{\beta 2}}{i_{\beta 1} - i_{\beta 2}}\right). \tag{9}$$

C. ANN BASED DEAD-TIME VOLTAGE COMPENSATION METHOD

After the maximum dead-time compensation voltage is obtained, an adaptive law is proposed. The magnitude of the compensated voltage vector is expressed as:

$$\begin{aligned} V_s^2 &= V_{ar}^2 + V_{\beta r}^2 \\ &= (V_\alpha - \Delta V_\alpha)^2 + (V_\beta - \Delta V_\beta)^2, \end{aligned} \tag{10}$$

where V_α and V_β are the reference voltages in α-β axes, $V_{\alpha r}$ and $V_{\beta r}$ are the voltages after compensation in α-β axes.

In order to obtain a stable self-reference voltage, a low-pass filter is used. The magnitude of the self-reference voltage vector is expressed as:

$$V_{ref}^2 = \frac{1}{1 + T_f^S} V_s^2, \tag{11}$$

where T_f is the filter time constant.

The voltage error is expressed as (12) according to (10) and (11):

$$V_{error} = V_{ref}^2 - V_s^2. \tag{12}$$

Considering the differences of hardware parameters are small, $w_a = w_b = w_c = w$. The adaptive law of the weight value is obtained as (13) according to the error backpropagation rule and the chain derivation rule:

$$\begin{aligned}\Delta w &= -\eta \frac{\partial(\frac{1}{2}V_{error}^2)}{\partial w} \\ &= -\eta V_{error}[\frac{2V_d}{3}V_{\alpha r}(2\frac{\partial f(i_a)}{\partial w} - \frac{\partial f(i_b)}{\partial w} \\ &\quad - \frac{\partial f(i_c)}{\partial w}) + \frac{2\sqrt{3}V_d}{3}V_{\beta r}(\frac{\partial f(i_b)}{\partial w} - \frac{\partial f(i_c)}{\partial w})] \\ &= -\eta V_{error}(l + m - n),\end{aligned} \tag{13}$$

where η is the learning factor. It affects the convergence speed of w. The expressions of l, m, and n are shown as follows:

$$\begin{cases} l = \dfrac{4V_{\alpha r}V_d}{3}\dfrac{\partial f(i_a)}{\partial w} \\ \quad = \dfrac{4V_{\alpha r}V_d}{3} \times \dfrac{2i_a e^{-wi_a}}{(1+e^{-wi_a})^2} \\ m = \dfrac{2\sqrt{3}\,V_{\beta r}V_d - 2V_{\alpha r}V_d}{3}\dfrac{\partial f(i_b)}{\partial w} \\ \quad = \dfrac{2\sqrt{3}\,V_{\beta r}V_d - 2V_{\alpha r}V_d}{3} \times \dfrac{2i_b e^{-wi_b}}{(1+e^{-wi_b})^2} \\ n = \dfrac{2\sqrt{3}\,V_{\beta r}V_d + 2V_{\alpha r}V_d}{3}\dfrac{\partial f(i_c)}{\partial w} \\ \quad = \dfrac{2\sqrt{3}\,V_{\beta r}V_d + 2V_{\alpha r}V_d}{3} \times \dfrac{2i_c e^{-wi_c}}{(1+e^{-wi_c})^2}. \end{cases} \tag{14}$$

Therefore, the adaptive law of the weight value is obtained as:

$$\begin{aligned} w(k) &= w(k-1) + \Delta w \\ &= w(k-1) - \eta V_{error}(l + m - n). \end{aligned} \tag{15}$$

According to the proposed ANN structure, the motor phase voltages in α-β axes are obtained after the dead-time voltage is compensated. Considering that only one parameter needs to be identified, the ANN structure mentioned before is simplified to a three-layer ANN structure. The control block diagram is shown in Fig. 5. When motor is running, the ANN algorithm is used to identify the nonlinear function of dead-time voltage in α-β coordinate system. The weight value is modified according to (15) continuously. A new reference voltage is obtained by the difference between the reference voltage and the dead-time compensation voltage. Therefore, the compensated reference voltages are approximated as the actual phase voltages on the motor side.

In order to implement the dead-time voltage compensation method without any system parameters, the above algorithm needs to be executed as follows:

I. When the motor is at standstill, the maximum dead-time compensation voltage is calculated according to the two-step voltage method and (9).

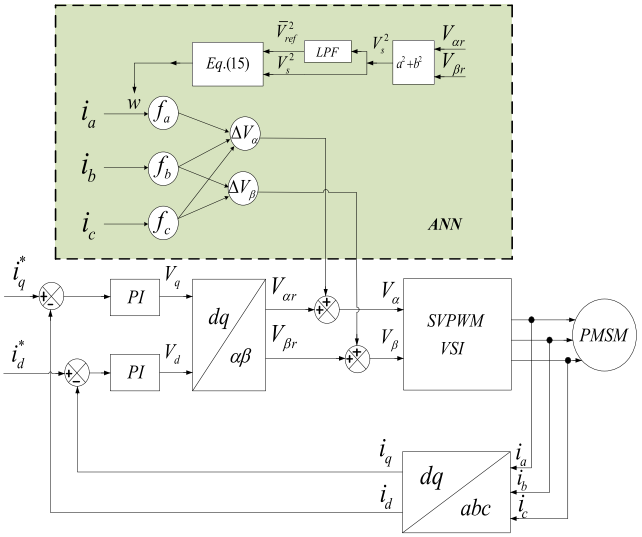

FIGURE 5. The control block diagram of dead-time voltage compensation method based on ANN.

II. When the motor is running, the nonlinear function of dead-time voltage is identified according to the ANN algorithm. The maximum dead-time compensation voltage used in the ANN algorithm is obtained by the step I.

D. CURRENT PREDICTIVE CONTROL

In the current loop, there is one-beat delay between the output voltages and currents due to the sampling delay and the calculation delay. According to the above analysis, the reference voltages are used to replace the phase voltages after compensation. Therefore, it is possible to use the reference voltages to predict one-beat currents to eliminate the mentioned delay. The α-β axes voltage equations are given as follows:

$$\begin{cases} V_\alpha = Ri_\alpha + L\dfrac{di_\alpha}{dt} + e_\alpha \\ V_\beta = Ri_\beta + L\dfrac{di_\beta}{dt} + e_\beta, \end{cases} \tag{16}$$

where R is the stator resistance, L is the stator inductance, V_α, V_β, i_α, and i_β are the α-β axes stator voltages and currents, respectively. e_α and e_β are the α-β axes back electromotive force, which is calculated by motor speed, flux linkage, and electrical angle.

The predicted currents are obtained as (17) according to (16):

$$\begin{cases} \hat{i}_\alpha(k+1) = i_\alpha(k) + \dfrac{T_s}{L}[V_{\alpha r}(k) - e_\alpha(k) - Ri_\alpha(k)] \\ \hat{i}_\beta(k+1) = i_\beta(k) + \dfrac{T_s}{L}[V_{\beta r}(k) - e_\beta(k) - Ri_\beta(k)], \end{cases} \tag{17}$$

where the reference voltages are used to replace the phase voltages.

The predictive currents are used as the feedback currents in the current loop in this paper. This will reduce the delay of the feedback currents and improve the response capability of the current loop.

TABLE 2. Parameters of testing PMSM and inverter.

Symbol	Quantity	Value
R	stator resistance	1.86Ω
L	stator inductance	$2.8\text{x}10^{-3}$H
Φ	magnetic flux	0.109Wb
n_p	pole-pairs number	4
T_d	dead time	3us
V_{dc}	dc link	310V
P	rated power	750W
f_s	switch frequency	12kHz

IV. EXPERIMENT RESULTS

The proposed compensation method is implemented in an ARM MCU (KV3125612). The main frequency of the MCU is 120MHz. The control cycle is 83.3us. And the computing time of the ANN method is 9.5us. Therefore, it accounts for 11.4% of the control cycle. The parameters of testing permanent magnet synchronous motor (PMSM) and inverter are shown in Table 2. The intelligent power module (FSBB30CH60F) is used as the power devices, which is the inverter module of IGBTs. The switch frequency of IGBTs is generally selected from 8khz to 16kHz. When the switch frequency is increased, the heat dissipation capacity is need to be increased due to the increase of switch loss. On the other hand, when the switch frequency is decreased, the harmonics of the current are increased due to the decrease of carrier ratio. Therefore, the switching frequency is selected as 12kHz in this paper. The dead-time in each switching period is set to 3us according to the recommendation of the intelligent power module (IPM). The experiment platform is shown in Fig. 6. A constant loading platform is used to control the load level. The rated-power of the tested VSI is 750W, and the DC link is 310V.

A. DEAD-TIME COMPENSATION VOLTAGE RESULTS

Fig. 7 shows the voltage and current waveforms of the two-step voltage experiment. The experimental data are recorded in flash and transmitted through serial communication when the test system is running. Firstly, the output of V_β is 12.6V, and the measured i_β is 1.476A. At 0.067s, the V_β is increased to 14.4V, and the measured i_β is 2.495A. V_d is calculated as 8.65V according to (9). After the maximum dead-time compensation voltage is obtained, only the weight value needs to be identified by the ANN algorithm.

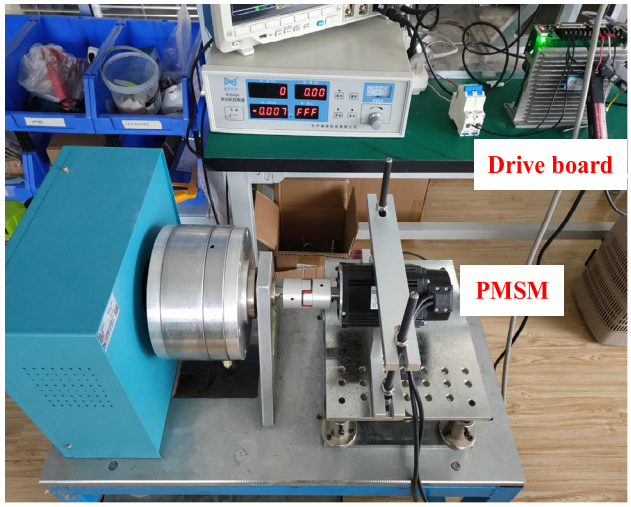

FIGURE 6. Hardware test platform.

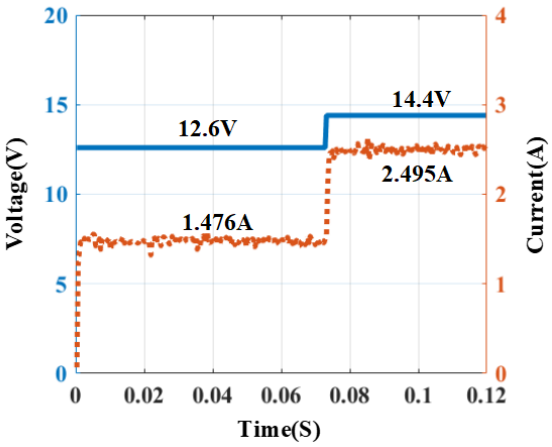

FIGURE 7. Voltage and current waveforms of two-step voltage method. (Experimental data are obtained by serial communication).

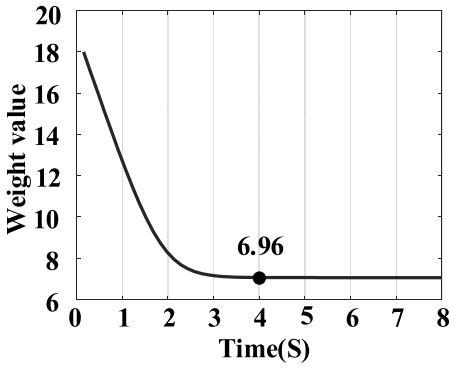

FIGURE 8. The waveform of weight value correction process. (Experimental data are obtained by serial communication).

Fig. 8 shows the correction process of the weight value. The weight value tends to a stable value of 6.96 at 4s, where the learn factor is 0.02. Since the nonlinear effects of inverters are not affected by the load torque and motor speed, the weight value remains constant under different working conditions. Therefore, the nonlinear function of dead-time compensation voltage is obtained.

After the nonlinear function is obtained, the voltages with compensation and without compensation are shown in Fig. 9. The compensation method with the sign function is selected as a comparison. The waveforms of voltages before compensation are distorted. This results in a voltage mismatch between the reference voltages and phase voltages. Using the reference voltages as the phase voltages for calculation will cause the performance degradation or even failure. The

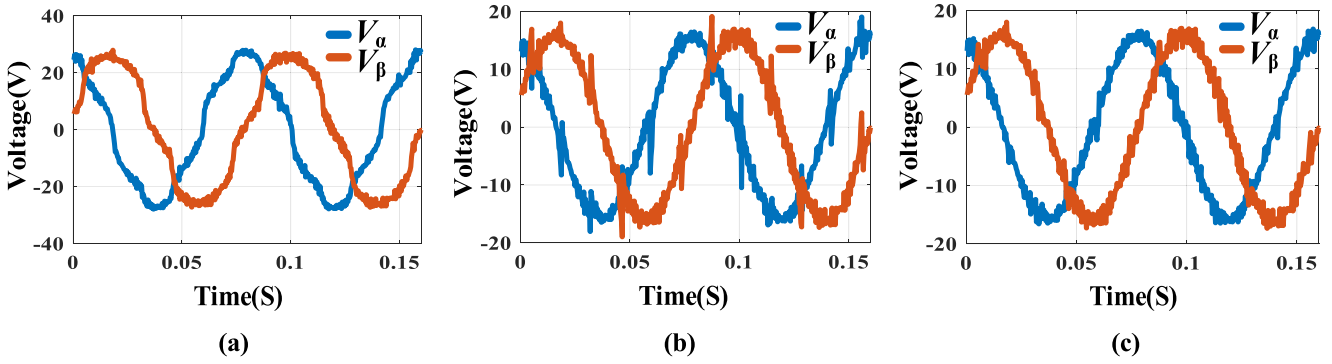

FIGURE 9. The voltage waveforms of (a) uncompensated method, (b) compensation method with the sign function, (c) compensation method with the proposed function. (Experimental data are obtained by serial communication).

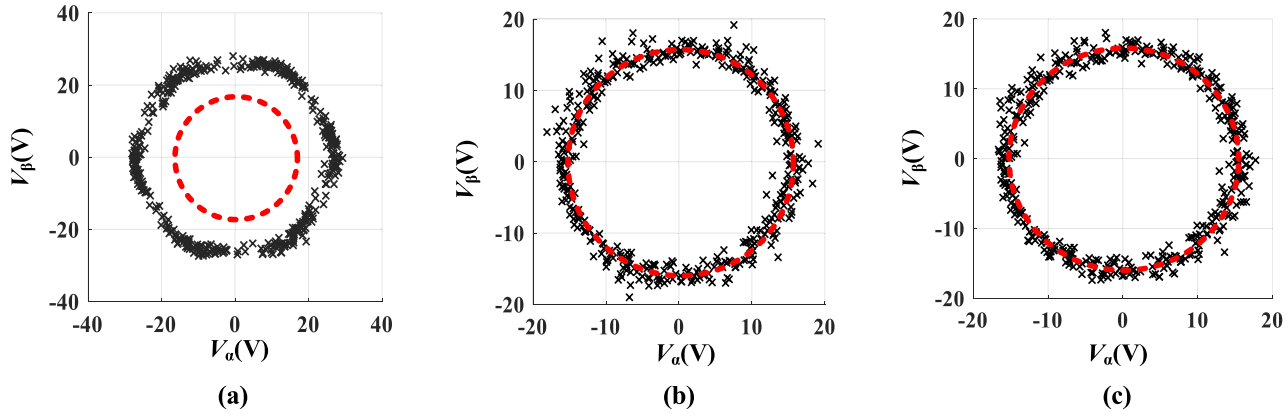

FIGURE 10. The *xy* plot of (a) uncompensated method, (b) compensation method with the sign function, (c) compensation method with the proposed function. (Experimental data are obtained by serial communication).

voltage distortions are reduced by the compensation method with the sign function. However, the discontinuities and burred feature show up in the current zero-crossing region, which degrades the compensation effect. Since the compensation voltage in the proposed function changes continuously with the phase currents in the zero-crossing region, the voltage distortions, discontinuities, and burred feature of the voltage waveforms are greatly reduced by the proposed method. The waveforms of voltages compensated by the two compensation methods are much closer to sinusoidal waveforms. This indicates that the compensated reference voltages can be approximated as the phase voltages.

Fig. 10 shows the *xy* plot waveforms of different compensation method. The red circular curves in Fig. 10 are the theoretical voltage vector trajectory at 200rpm (16.5V). The scattered point waveforms of the voltages compensated by the two compensation methods are closer to the theoretical circular trajectory. This shows that the magnitude of the voltage vector after compensation is a constant value. This fits the proposed theoretical assumption of weight value correction rule. However, there are some points away from the theoretical circle, when the voltage is compensated by the compensation method with the sign function. It is caused by the discontinuity of the sign function in the zero-crossing region. Nevertheless, the points are much closer to the theoretical circle, when the voltage is compensated by the proposed method. Therefore, the voltage mismatch between the reference voltages and the output voltages is greatly reduced by the proposed method. And the actual phase voltages are obtained without adding any hardware.

B. CURRENT COMPENSATION RESULTS

Fig. 11 shows the current waveforms of different compensation methods. The current distortions are reduced by the two compensation methods. However, due to the sudden change of the sign function in the current zero-crossing region, the change of currents in the zero-crossing region is discontinuous. Both the current distortions and the discontinuous phenomenon are greatly reduced by the compensation method with the proposed function. Fig. 12 shows the Fast Fourier Transform (FFT) results of different compensation methods. The current harmonics caused by the nonlinear effects of inverters are mainly the 5^{th} and 7^{th} harmonics. The total harmonic distortion (THD) of the uncompensated current waveforms is 7.91%.

The 5^{th} and 7^{th} harmonics are suppressed by the two compensation methods. However, the higher harmonics as 6^{th}, 8^{th}, and 10^{th} are increased by the compensation method

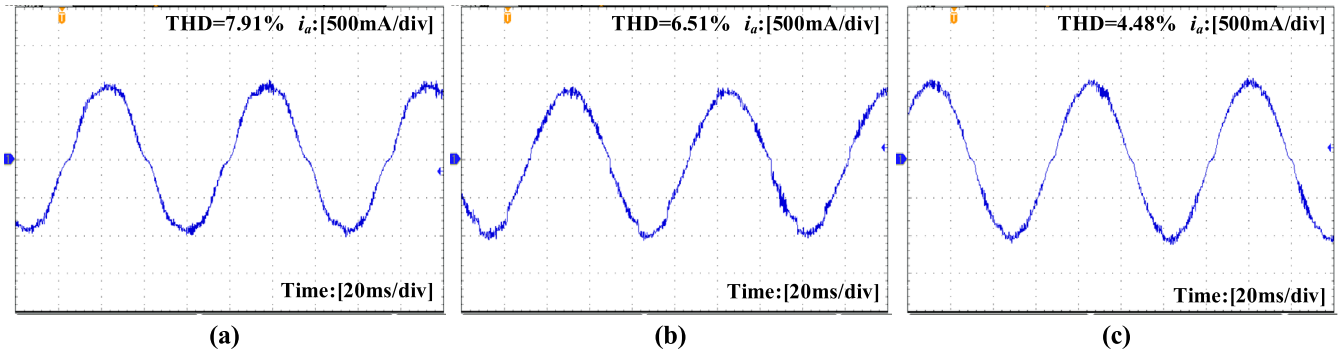

FIGURE 11. The current waveforms of (a) uncompensated method, (b) compensation method with the sign function, (c) compensation method with the proposed function. (Experimental data are obtained by an oscilloscope).

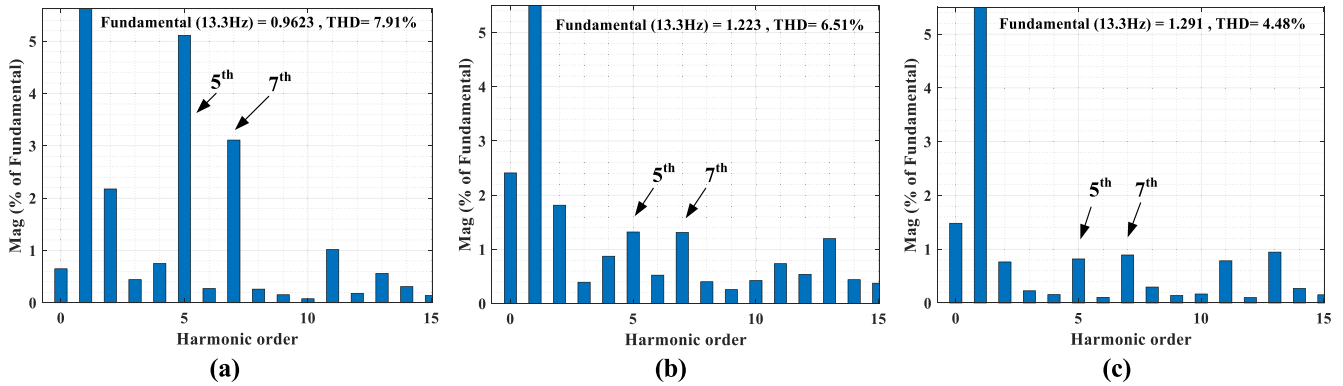

FIGURE 12. The FFT results of (a) uncompensated method, (b) compensation method with the sign function, (c) compensation method with the proposed function. (Experimental data are obtained by an oscilloscope).

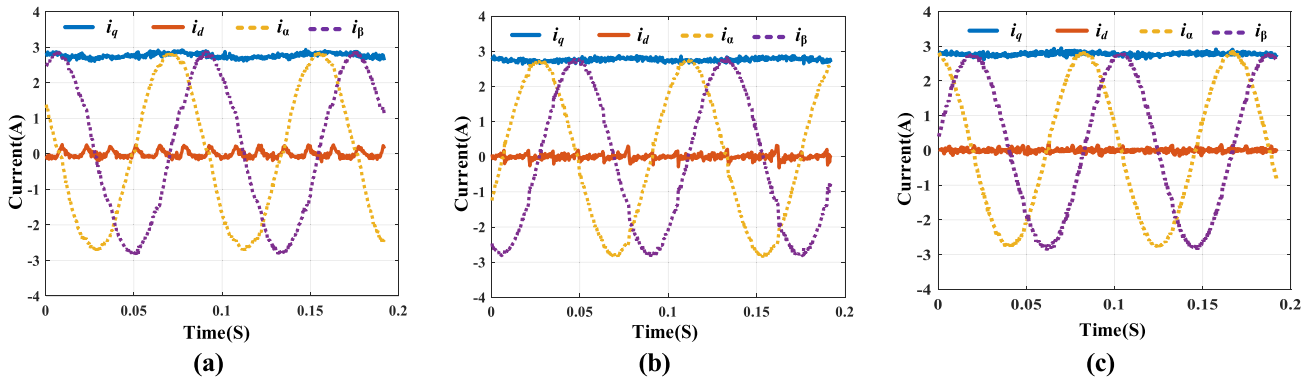

FIGURE 13. The current waveforms of (a) uncompensated method, (b) compensation method with the sign function, and (c) compensation method with the proposed function. (Experimental data are obtained by serial communication).

with the sign function. This is caused by the discontinuous change of currents in the zero-crossing region. When the voltage mismatch is compensated by the proposed method, the harmonic components mentioned above are not increased. Therefore, the current distortions are significantly reduced by the proposed compensation method, and the THD is also reduced from 7.91% to 4.48%.

Fig. 13 shows the current waveforms of different compensation methods in the α-β coordinate system and the d-q coordinate system. The id = 0 control method is used. The 6^{th} harmonic is quite large in the d-axis current waveforms, which is caused by the nonlinear effects of inverters. The 6^{th} harmonic is suppressed by the two compensation methods. However, by using the proposed compensation method, the sixth harmonic component is significantly reduced. At the same time, the 6^{th} harmonic component in the compensated q-axis current is quite small. Therefore, torque fluctuations due to inverter nonlinear effects are reduced by the proposed

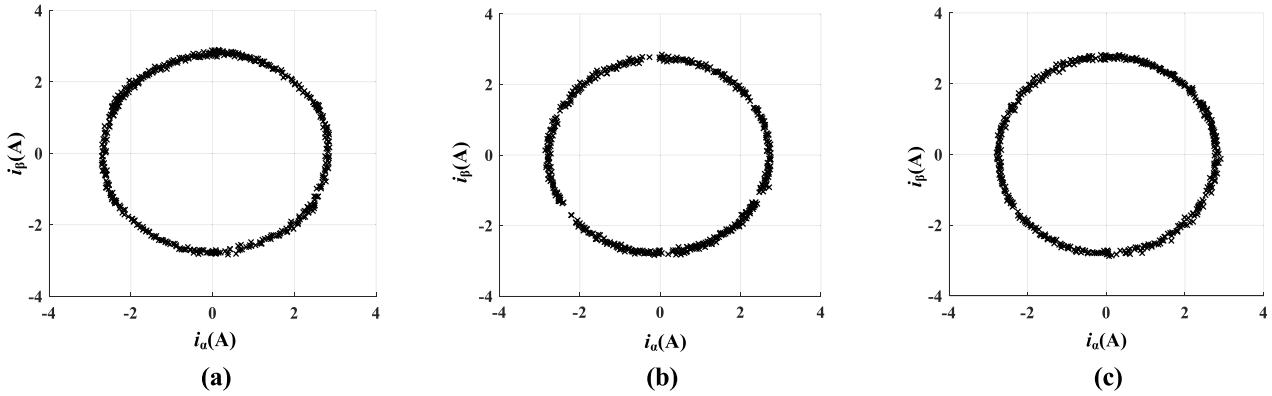

FIGURE 14. The xy plot current waveforms of (a) uncompensated method, (b) compensation method with the sign function, and (c) compensation method with the proposed function. (Experimental data are obtained by serial communication).

compensation method. Fig. 14 shows the xy plot current waveforms of different compensation methods in the α-β coordinate system. The compensated current trajectory is much closer to a circle than the uncompensated current trajectory. This indicates that the current distortions are reduced by the two compensation methods. When currents are compensated by the method with the sign function, the discontinuities show up in the current zero-crossing region. This also shows that using this method will cause the discontinuous change of currents in the zero-crossing region. The trajectory of the current compensated by the proposed method is a continuous circle. Therefore, the current distortions are significantly reduced by the proposed method both in the α-β coordinate system and the d-q coordinate system.

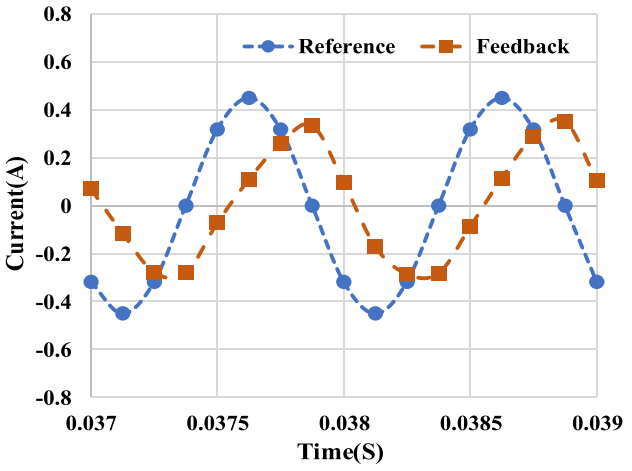

FIGURE 15. Response waveforms of the normal current loop under 1500Hz excitation. (Experimental data are obtained by serial communication).

Fig. 15 shows the current waveforms of the normal current loop under 1500Hz excitation. The phase lag between the reference current and the feedback current is almost 90 degrees. This means that the bandwidth of the current loop is 1500Hz. Fig. 16 shows the current waveforms of the proposed current loop under 2000Hz excitation. The phase lag between the

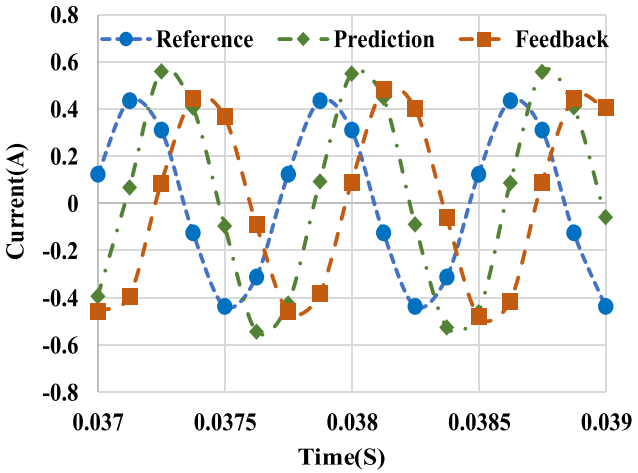

FIGURE 16. Response waveforms of the proposed current loop under 2000Hz excitation. (Experimental data are obtained by serial communication).

reference current and the predictive current is 45 degrees. But the phase lag between the reference current and the feedback current is 90 degrees. Therefore, the bandwidth of the proposed current loop is 2000Hz. Through the above analysis, the bandwidth of the proposed current loop is increased by 500Hz.

V. CONCLUSION

This paper proposes a dead-time voltage compensation method based on ANN. The non-linear model of dead-time compensation voltage is obtained through online identification. The voltage mismatch is significantly reduced by the proposed method. Applying this method to the current predictive control, the bandwidth of the current loop is increased by 500Hz. The experimental results show that the current distortions due to the nonlinear effects of inverters are reduced and the THD of currents is reduced from 7.91% to 4.48%. Therefore, the phase voltages are obtained accurately and

the current distortions are greatly reduced by the proposed method without adding any hardware.

REFERENCES

[1] J.-W. Choi and S.-K. Sul, "Inverter output voltage synthesis using novel dead time compensation," *IEEE Trans. Power Electron.*, vol. 11, no. 2, pp. 221–227, Mar. 1996, doi: 10.1109/63.486169.

[2] J.-S. Choi, J.-Y. Yoo, S.-W. Lim, and Y.-S. Kim, "A novel dead time minimization algorithm of the PWM inverter," in *Proc. IEEE Ind. Appl. Conf.*, Phoenix, AZ, USA, May 1999, pp. 2188–2193, doi: 10.1109/IAS.1999.798757.

[3] X. Song, X. Wen, X. Guo, and F. Zhao, "Dead-time compensation of SVPWM based on DSP TMS320F2812 for PMSM," in *Proc. Int. Conf. Electr. Mach. Syst.*, Tokyo, Japan, Nov. 2009, pp. 1–4, doi: 10.1109/ICEMS.2009.5382971.

[4] Y. Park and S.-K. Sul, "A novel method utilizing trapezoidal voltage to compensate for inverter nonlinearity," *IEEE Trans. Power Electron.*, vol. 27, no. 12, pp. 4837–4846, Dec. 2012, doi: 10.1109/TPEL.2012.2192451.

[5] Z. Zhang and L. Xu, "Dead-time compensation of inverters considering snubber and parasitic capacitance," *IEEE Trans. Power Electron.*, vol. 29, no. 6, pp. 3179–3187, Jun. 2014, doi: 10.1109/TPEL.2013.2275551.

[6] N. Bedetti, S. Calligaro, and R. Petrella, "Self-commissioning of inverter dead-time compensation by multiple linear regression based on a physical model," *IEEE Trans. Ind. Appl.*, vol. 51, no. 5, pp. 3954–3964, Sep. 2015, doi: 10.1109/TIA.2015.2436882.

[7] W. Chen, B. Li, D. Xu, and L. Cai, "A dead-time compensation method for voltage source inverters," in *Proc. 22nd Int. Conf. Electr. Mach. Syst. (ICEMS)*, Harbin, China, Aug. 2019, pp. 1–6, doi: 10.1109/ICEMS.2019.8921871.

[8] S.-Y. Kim, W. Lee, M.-S. Rho, and S.-Y. Park, "Effective dead-time compensation using a simple vectorial disturbance estimator in PMSM drives," *IEEE Trans. Ind. Electron.*, vol. 57, no. 5, pp. 1609–1614, May 2010, doi: 10.1109/TIE.2009.2033098.

[9] T. V. Swathy and T. V. Abhilash, "High performance vector control of PMSM with dead-time compensation," in *Proc. IEEE Int. Conf. Power Electron., Drives Energy Syst. (PEDES)*, Bengaluru, Karnataka, Dec. 2012, pp. 1–6, doi: 10.1109/PEDES.2012.6484464.

[10] G. Liu, D. Wang, Y. Jin, M. Wang, and P. Zhang, "Current-detection-independent dead-time compensation method based on terminal voltage A/D conversion for PWM VSI," *IEEE Trans. Ind. Electron.*, vol. 64, no. 10, pp. 7689–7699, Oct. 2017, doi: 10.1109/TIE.2017.2696480.

[11] S. Zhu, W. Huang, and Y. Yan, "A simple inverter nonlinearity compensation method using on-line voltage error observer," in *Proc. 22nd Int. Conf. Electr. Mach. Syst. (ICEMS)*, Harbin, China, Aug. 2019, pp. 1–6, doi: 10.1109/ICEMS.2019.8921445.

[12] K. Liu and Z. Q. Zhu, "Online estimation of the rotor flux linkage and voltage-source inverter nonlinearity in permanent magnet synchronous machine drives," *IEEE Trans. Power Electron.*, vol. 29, no. 1, pp. 418–427, Jan. 2014, doi: 10.1109/TPEL.2013.2252024.

[13] D. Liang, J. Li, R. Qu, and W. Kong, "Adaptive second-order sliding-mode observer for PMSM sensorless control considering VSI nonlinearity," *IEEE Trans. Power Electron.*, vol. 33, no. 10, pp. 8994–9004, Oct. 2018, doi: 10.1109/TPEL.2017.2783920.

[14] D. Yu, J. Xia, Y. Guo, and X. Zhang, "Super-twisting sliding mode observer-based IPMSM sensorless control strategy considering VSI nonlinearity," in *Proc. 22nd Int. Conf. Electr. Mach. Syst. (ICEMS)*, Harbin, China, Aug. 2019, pp. 1–6, doi: 10.1109/ICEMS.2019.8921755.

[15] H.-S. Ryu, I.-H. Lim, J.-H. Lee, S.-H. Hwang, and J.-M. Kim, "A dead time compensation method in voltage-fed PWM inverter," in *Proc. IEEE Ind. Appl. Conf.*, Tampa, FL, USA, Oct. 2006, pp. 911–916, doi: 10.1109/IAS.2006.256633.

[16] J. M. Guerrero, M. Leetmaa, F. Briz, A. Zamarron, and R. D. Lorenz, "Inverter nonlinearity effects in high-frequency Signal-Injection-Based sensorless control methods," *IEEE Trans. Ind. Appl.*, vol. 41, no. 2, pp. 618–626, Mar. 2005, doi: 10.1109/TIA.2005.844411.

[17] S.-H. Hwang and J.-M. Kim, "Dead time compensation method for voltage-fed PWM inverter," *IEEE Trans. Energy Convers.*, vol. 25, no. 1, pp. 1–10, Mar. 2010, doi: 10.1109/TEC.2009.2031811.

[18] T. Qiu, X. Wen, and F. Zhao, "Adaptive-Linear-Neuron-Based dead-time effects compensation scheme for PMSM drives," *IEEE Trans. Power Electron.*, vol. 31, no. 3, pp. 2530–2538, Mar. 2016, doi: 10.1109/TPEL.2015.2427914.

[19] Z. Tang and B. Akin, "A new LMS algorithm based deadtime compensation method for PMSM FOC drives," *IEEE Trans. Ind. Appl.*, vol. 54, no. 6, pp. 6472–6484, Nov. 2018, doi: 10.1109/TIA.2018.2853045.

[20] M. Kumar, "Time-domain characterization of digitized PWM inverter with dead-time effect," *IEEE Trans. Circuits Syst. I, Reg. Papers*, vol. 65, no. 10, pp. 3592–3601, Oct. 2018, doi: 10.1109/TCSI.2018.2827950.

[21] N. Jiao, S. Wang, T. Liu, Y. Wang, and Z. Chen, "Harmonic quantitative analysis for dead-time effects in SPWM inverters," *IEEE Access*, vol. 7, pp. 43143–43152, 2019, doi: 10.1109/ACCESS.2019.2907176.

[22] U. Abronzini, C. Attaianese, M. D'Arpino, M. Di Monaco, and G. Tomasso, "Steady-state dead-time compensation in VSI," *IEEE Trans. Ind. Electron.*, vol. 63, no. 9, pp. 5858–5866, Sep. 2016, doi: 10.1109/TIE.2016.2586680.

[23] C. Attaianese and G. Tomasso, "Predictive compensation of dead-time effects in VSI feeding induction motors," *IEEE Trans. Ind. Appl.*, vol. 37, no. 3, pp. 856–863, 2001, doi: 10.1109/28.924768.

[24] Y. Li, Z. Zhang, K. Li, P. Zhang, and F. Gao, "Predictive current control for voltage source inverters considering dead-time effect," *CES Trans. Electr. Mach. Syst.*, vol. 4, no. 1, pp. 35–42, Mar. 2020, doi: 10.30941/CES-TEMS.2020.00006.

[25] L. Ben-Brahim, A. Gastli, and K. Ghazi, "Implementation of iterative learning control based deadtime compensation for PWM inverters," in *Proc. 17th Eur. Conf. Power Electron. Appl. (EPE ECCE-Europe)*, Geneva, Switzerland, Sep. 2015, pp. 1–8, doi: 10.1109/EPE.2015.7311779.

[26] L. Ben-Brahim, "On the compensation of dead time and zero-current crossing for a PWM-inverter-controlled AC servo drive," *IEEE Trans. Ind. Electron.*, vol. 51, no. 5, pp. 1113–1118, Oct. 2004, doi: 10.1109/TIE.2004.834940.

[27] L. Ben-Brahim, "Iterative learning control for variable frequency drives," in *Proc. IEEE Power Electron. Specialists Conf.*, Rhodes, Greece, Jun. 2008, pp. 617–623, doi: 10.1109/PESC.2008.4591998.

[28] Z. Tang and B. Akin, "Suppression of dead-time distortion through revised repetitive controller in PMSM drives," *IEEE Trans. Energy Convers.*, vol. 32, no. 3, pp. 918–930, Sep. 2017, doi: 10.1109/TEC.2017.2679701.

[29] O. I. Abiodun, M. U. Kiru, A. Jantan, A. E. Omolara, K. V. Dada, A. M. Umar, O. U. Linus, H. Arshad, A. A. Kazaure, and U. Gana, "Comprehensive review of artificial neural network applications to pattern recognition," *IEEE Access*, vol. 7, pp. 158820–158846, 2019, doi: 10.1109/ACCESS.2019.2945545.

[30] A. Yang, Y. Zhuansun, C. Liu, J. Li, and C. Zhang, "Design of intrusion detection system for Internet of Things based on improved BP neural network," *IEEE Access*, vol. 7, pp. 106043–106052, 2019, doi: 10.1109/ACCESS.2019.2929919.

[31] X. Zhang, C. Feng, R. Li, J. Lei, and C. Tang, "NeuralTaint: A key segment marking tool based on neural network," *IEEE Access*, vol. 7, pp. 68786–68798, 2019, doi: 10.1109/ACCESS.2019.2915681.

TAO LIU was born in Hebei, China, in 1994. He received the B.Eng. degree from Xiamen University, Xiamen, China, in 2017, and the M.Eng. degree from the Huazhong University of Science and Technology, Wuhan, China, in 2019, where he is currently pursuing the Ph.D. degree with the School of Optical and Electronic Information.

His current research interests include control of permanent-magnet synchronous machine drives and compensation of voltage-source inverter nonlinearity.

QIDONG LI received the B.E. degree in electronic engineering from the Huazhong University of Science and Technology, Wuhan, Hubei, China, in 2016, where he is currently pursuing the Ph.D. degree with the School of Optical and Electronic Information.

His current research interests include sensorless control of permanent magnet synchronous machine drives and compensation of voltage-source inverter nonlinearity.

QIAOLING TONG (Member, IEEE) received the B.Eng. and Ph.D. degrees from the School of Optical and Electronic Information, Huazhong University of Science and Technology, China, in 2003 and 2010, respectively. From 2008 to 2010, he was a Research Scholar with the Department of Electrical Engineering and Computer Science, University of California at Irvine, Irvine. He is currently an Associate Professor with the School of Optical and Electronic Information, Huazhong University of Science and Technology. His current research interests include sensorless control of dc–dc converters and VLSI implementation of intelligent algorithms.

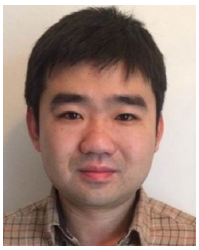

QIAO ZHANG (Member, IEEE) received the B.Eng., M.Eng., and Ph.D. degrees from the Huazhong University of Science and Technology, Wuhan, China, in 2003, 2006, and 2010, respectively. From 2008 to 2009, he was a Visiting Scholar with the Department of Electronic and Electrical Engineering, The University of Sheffield, U.K. From 2009 to 2016, he was a Research Engineer with the IMRA Europe U.K. Research Centre. He is currently an Associate Professor with the School of Automation, Wuhan University of Technology. His research interests include the power electronics system design and control, such as dc–dc converter sensorless control strategies, electrical machine parameters estimation by control theory, system nonlinearity compensation for dc–dc converters, and voltage source inverters.

KAN LIU (Senior Member, IEEE) received the B.Eng. and Ph.D. degrees in automation from Hunan University, Changsha, China, in 2005 and 2011, respectively, and the Ph.D. degree in electronic and electrical engineering from The University of Sheffield, Sheffield, U.K., in 2013.

From 2013 to 2016, he was a Research Associate with the Department of Electronic and Electrical Engineering, The University of Sheffield. From 2016 to 2017, he was a Lecturer with the Control Systems Group, Loughborough University. He is currently a Professor of electro-mechanical engineering with Hunan University. He is also the Director of the Engineering Research Center of Ministry of Education on Automotive Electronics and Control Technology, China. His research interests include parameters estimation and sensorless control of permanent magnet synchronous machine drives, advanced design, and control solutions of high-power density converters, for applications ranging from electric locomotive and automotive, to servo motor, and drive.

Prof. Liu serves as an Associate Editor for IEEE Access and the *CES Transactions on Electrical Machines and Systems*.